For two opposite-phase waves of unit amplitude incident on arms 1 and 4, the reflected waves for the odd mode are

$$b_{1o} = -b_{4o} = S_{11o} \tag{46}$$

$$b_{3o} = -b_{2o} = S_{12o}. \tag{47}$$

Adding the even and odd modes together, we have the resultant incident and reflected waves

$$a_1 = 2 \tag{48}$$

$$b_1 = b_{1e} + b_{1o} = S_{11e} + S_{11o} \tag{49}$$

$$b_2 = b_{2e} + b_{2o} = S_{12e} - S_{12o} \tag{50}$$

$$b_3 = b_{3e} + b_{3o} = S_{12e} + S_{12o} \tag{51}$$

$$b_4 = b_{4e} + b_{4o} = S_{11e} - S_{11o}. \tag{52}$$

Similarly, for waves incident on arms 2 and 3, we have for the resultant incident and reflected waves

$$a_3 = 2 \tag{53}$$

$$b_1 = S_{12e} + S_{12o} \tag{54}$$

$$b_2 = S_{22e} - S_{22o} \tag{55}$$

$$b_3 = S_{22e} + S_{22o} \tag{56}$$

$$b_4 = S_{12e} - S_{12o}. \tag{57}$$

ACKNOWLEDGMENT

The author wishes to acknowledge Dr. J. Carpenter, F. Hennessey and A. B. Hadik-Barkóczy for their helpful suggestions concerning this paper.

A Coupled Strip-Line Configuration Using Printed-Circuit Construction that Allows Very Close Coupling*

WILLIAM J. GETSINGER†, MEMBER, IRE

Summary—A new strrip-line configuration is presented, applicable to printed-circuit construction, that allows very close coupling to be achieved without esorting to very small coupling gaps and excessively critical dimensions. Graphs of even- and odd-mode fringing capacitances are given. These graphs can be used with simple formulas, which also are given, to determine the dimensions of the configuration that will give specified even- and odd-mode characteristic impedances or shunt capacitances.

The usefulness of the graphs and formulas was demonstrated by using them to design 3-db backward-couplers. The performance of the couplers in this new configuration was typical of similar couplers made in more conventional configurations, as expected. However, the devices shown have an advantage in that they can be manufactured by relatively inexpensive and rapid printed-circuit methods and, since the region between the conductors is solid dielectric, they are unusually rugged.

I. GENERAL

IN working with shielded strip-line, the need for closely coupled strips arises in designing 3-db couplers [1] and broad-band filters [2], [3]. The typical printed-circuit coupled strip-line configuration consists of two slabs of dielectric sandwiched between parallel ground planes. One of the slabs has two parallel copper strips printed on it. Coupling is achieved by bringing adjacent edges of the two strips close enough to cause appreciable capacitance to exist between the strips. Very close coupling requires that the strips be brought very near each other. For the 3-db coupler, and even more for very broad-band parallel-coupled filters, the spacing between strips becomes too small to be made accurately using practical construction techniques because the allowable tolerance on the spacing decreases as the spacing decreases. Thus, there is a practical limit to the inter-strip capacitance that can be achieved with edge-coupled thin strips.

One solution to this problem has been to orient the coupled strips face-to-face and perpendicular to the ground planes. While this achieves large inter-strip capacitance, it is not always a desirable configuration, because it is difficult to build and it does not interconnect easily with more conventional strip-line circuits in which the strip is parallel to the ground planes. Also, current tends to concentrate at the thin edges of the strips in this construction, causing higher losses.

It is also possible to use thick bars for strips in order to achieve sufficient inter-strip capacitance, but this

* Received by the PGMTT, June 2, 1961; revised manuscript received, July 7, 1961. This work was supported by the U. S. Army Signal Research and Development Laboratory, Fort Monmouth, N. J., as part of Contract DA 36-039 SC-74862, Sub-Task 3-26-01-701, DA Project 3-26-01-000.

† Electromagnetics Laboratory, Stanford Research Institute, Menlo Park, Calif.

possibility precludes the use of printed-circuit materials and techniques.

II. Proposed Configuration

A cross section of coupled strip-lines using the proposed construction is shown in Fig. 1. The two strips denoted by c are tied together at the ends of the microwave component in which they are used, while in the coupling region, strips c overlap the strip denoted by a. Thus, strips c form a single transmission line coupled to the transmission line formed by strip a. Large coupling between these two lines is achieved by using the parallel-plate capacitance caused by the overlapping. This configuration uses thin strips parallel to the ground planes, and thus is amenable to the use of printed-circuit techniques and materials. It connects easily with conventional strip-line circuits, and does not require critical tolerances. This construction will be denoted by the term *interleaving*.

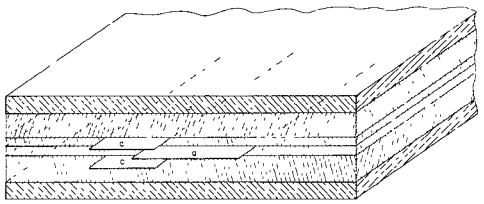

Fig. 1—Proposed strip-line configuration.

It is necessary to use a symmetrical construction with respect to the ground planes, requiring two outer center-strips for one line, in order to prevent radiation into a parallel-plate mode between the ground planes.

III. Technical Description

The characteristic impedance, Z_0, of a lossless uniform transmission line operating in the TEM mode is related to its shunt capacitance by:

$$Z_0\sqrt{\epsilon_r} = \frac{\eta}{(C/\epsilon)} \text{ ohms} \tag{1}$$

where

- $\sqrt{\epsilon_r}$ is the relative dielectric constant of the medium in which the wave travels
- η is the impedance of free space = 376.7 ohms per square
- C/ϵ is the ratio of the static capacitance per unit length between conductors to the permittivity (in the same units) of the dielectric medium. This ratio is independent of the dielectric constant.

The even- and odd-mode impedances of coupled TEM lines [4], [5] can be found by substituting even- and odd-mode capacitances of the lines into (1).

A generalized schematic diagram of shielded coupled-strip transmission line is shown in Fig. 2. The circles represent the coupled conductors. The capacitance to ground for a single conductor when both conductors are at the same potential is C_{oe}, the even-mode capacitance. The capacitance to ground when the two conductors are oppositely charged with respect to ground is C_{oo}, the odd-mode capacitance. It is assumed that the physical arrangement is such that the even-mode capacitances of the two conductors are the same, thus implying that the odd-mode capcitances are also the same. This paper relates these capacitances to the physical dimensions of the strips.

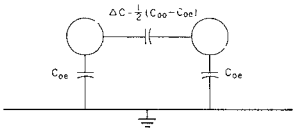

Fig. 2—Generalized schematic diagram.

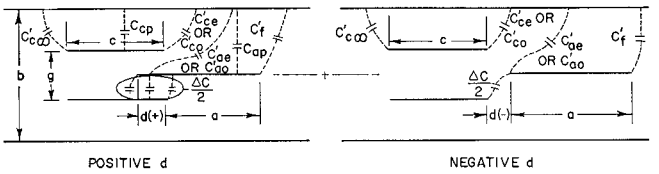

Fig. 3—Capacitances and dimension of proposed strip-line configuration.

The structure of Fig. 1 is composed of parallel planar surfaces. This makes it practical to consider the total capacitance of a given strip to be composed of parallel-plane capacitances plus appropriate fringing capacitances. (Fringing capacitances take into account the distortion of the field lines in the vicinity of the edges of the plane strips.) Fig. 3 relates the various capacitances to the geometry of the structure under consideration. Two diagrams are shown to clarify the definitions for strip a inserted in and withdrawn from strips c. All capacitances are defined on the basis of unit depth into the paper. The parallel-plane capacitances to one ground plane are given by:

$$\frac{C_{ap}}{\epsilon} = \frac{2a}{b} \tag{2}$$

$$\frac{C_{cp}}{\epsilon} = \frac{2c/b}{1 - g/b}. \tag{3}$$

Capacitance ΔC, between the center strips, has been plotted as a function of g/b and d/g in Fig. 4. The fringing capacitances were found by conformal mapping techniques. The derivations are given in the Appendix. Graphs of the fringing capacitances as functions of g/b and d/g are given in Figs. 5–9. Notice that the parallel-plate and fringing capcitances are defined to apply from one side of the center line to the nearest ground plane, as shown in Fig. 3.

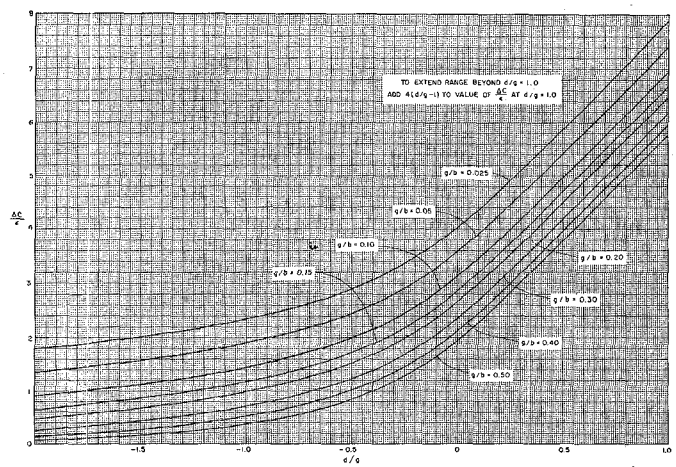

Fig. 4—Inter-strip capacitance.

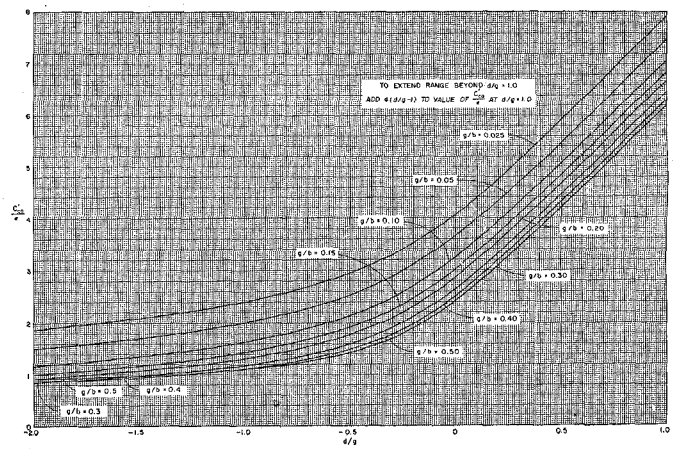

Fig. 7—Odd-mode fringing capacitance of strip *c*.

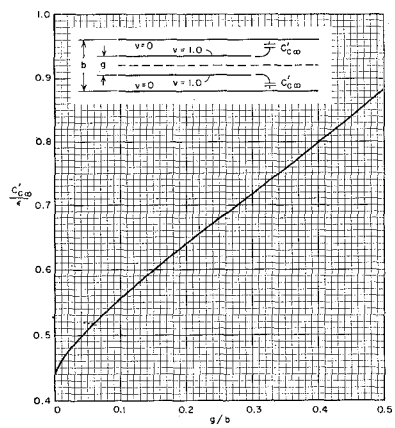

Fig. 5—Fringing capacitance of offset thin strip.

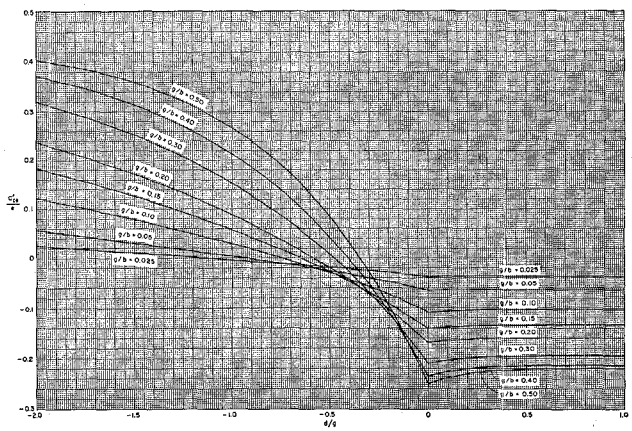

Fig. 8—Even-mode fringing capacitance of strip *a*.

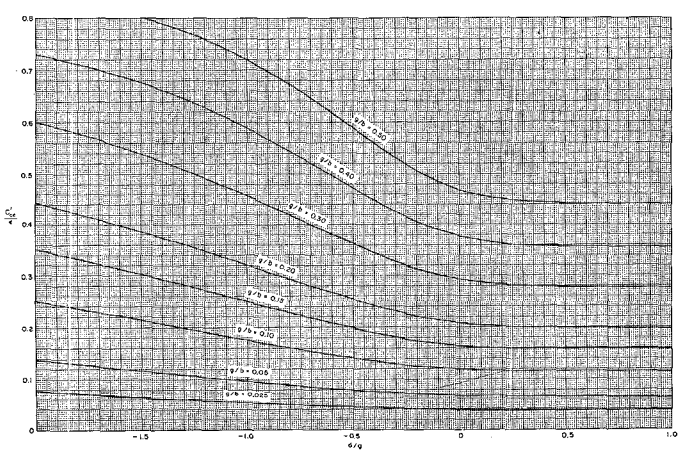

Fig. 6—Even-mode fringing capacitance of strip *c*.

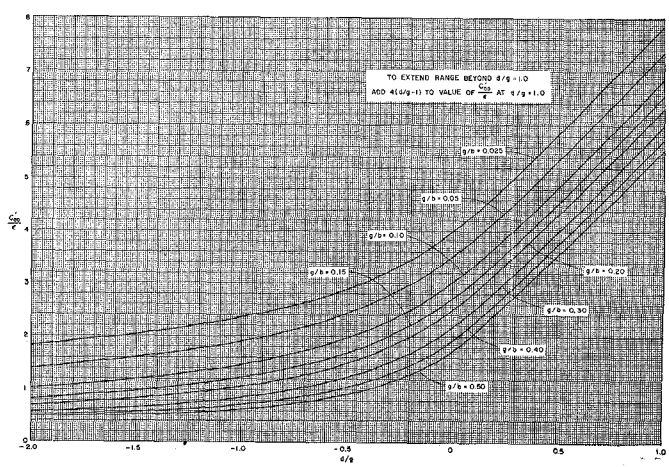

Fig. 9—Odd-mode fringing capacitance of strip *a*.

The total even-mode capacitance for either strip is given by the sum of all of the capacitances to ground associated with that strip when operating in the even mode:

$$C_{oe} = 2[C_{ae}' + C_f' + C_{ap}] = 2[C_{ce}' + C_{c\infty}' + C_{cp}]. \quad (4)$$

Eq. (4) imposes the condition that the even-mode capacitances be the same for the two transmission lines. Similarly,

$$C_{oo} = 2[C_{ao}' + C_f' + C_{ap}] = 2[C_{co}' + C_{c\infty}' + C_{cp}]. \quad (5)$$

When the strips are operating in the odd mode, they are oppositely charged, one positive and one negative, and thus a surface of zero potential exists somewhere between them. The odd-mode fringing capacitances include the capacitance (ΔC) to this wall of zero potential, as well as the capacitances to the actual ground plane.

When identical even-mode capacitances have been imposed on the two lines, it can be shown that the odd-mode capacitances are also the same. Subtraction of (4) from (5) gives

$$C_{oo} - C_{oe} = 2(C_{ao}' - C_{ae}') = 2(C_{co}' - C_{ce}'). \quad (6)$$

The total capacitance between the two lines is denoted ΔC and is given by

$$\Delta C = (1/2)(C_{oo} - C_{oe}). \quad (7)$$

This follows from consideration of the definitions of even- and odd-mode capacitances, as indicated on Fig. 2. The quantity $\Delta C/\epsilon$ is given as a function of d/g and g/b in Fig. 4. The capacitance C_f' is the same as $C_{c\infty}'$ at $g/b=0$, and its value is given by

$$\frac{C_f'}{\epsilon} = 0.441. \quad (8)$$

Through the use of the above relations and figures, it is possible to relate physical dimensions of the given configuration to even- and odd-mode capacitances or impedances.

IV. Use of the Graphs

Usually an engineer has already determined values of even- and odd-mode impedances, Z_{oe} and Z_{oo}, or even- and odd-mode capacitances, C_{oe} and C_{oo}, and wishes to determine the corresponding physical parameters. A simple procedure accomplishes this. Eq. (7) can be written

$$\Delta C/\epsilon = \frac{1}{2}\left(\frac{C_{oo}}{\epsilon} - \frac{C_{oe}}{\epsilon}\right). \quad (9)$$

Using (1) gives

$$\Delta C/\epsilon = \frac{\eta}{2\sqrt{\epsilon_r}}\left(\frac{1}{Z_{oo}} - \frac{1}{Z_{oe}}\right). \quad (10)$$

Values of b and g are selected, and then used with the value of $\Delta C/\epsilon$ found by (9) or (10) to determine d/g directly from the graph of Fig. 4. Next, having determined C_{oe}/ϵ from Z_{oe} and (1), it is possible to find $C_{c\infty}'/\epsilon$ and C_{ce}'/ϵ from Figs. 5 and 6. These quantities are substituted in (11) to give c/b:

$$c/b = \frac{1 - g/b}{2}\left[\frac{1}{2}C_{oe}/\epsilon - C_{c\infty}'/\epsilon - C_{ce}'/\epsilon\right]. \quad (11)$$

Finally, C_{ae}'/ϵ is found from Fig. 8 and substituted in (12) to give a/b.

$$a/b = \tfrac{1}{2}\left[\tfrac{1}{2}C_{oe}/\epsilon - C_{ae}'/\epsilon - 0.441\right]. \quad (12)$$

Thus, all the physical dimensions are determined. These formulas are accurate for $a/b>0.35$ and $(c/b)/(1-g/b)>0.35$. For narrower widths, simple corrections are possible which will be given in the next section.

Eqs. (11) and (12), used to determine c/b and a/b, were derived from (4) and use no odd-mode capacitances. Similar equations for determining a/b and c/b could have been derived using (5), and then no even-mode capacitances would have been involved. Both methods are equally valid. This paper includes graphs of both even- and odd-mode capacitances for completeness and for possible applications in which one mode may be of greater interest than another, although only the even-mode graphs, Figs. 6 and 8 will be used in the examples to follow.

In a specific device, the feeding lines connected to the coupled region may be constructed of single and dual strips in isolation from each other. The characteristic impedance of a single thin strip between parallel ground planes [6] is either the even- or odd-mode characteristic impedance of strip a when widely separated from strips c. Adding the fringing capacitances from the edges of a thin strip [see (8)] to the parallel plate capacitances from its surfaces [see (2)], and then substituting in (1) gives the following formula for the relative strip width a/b, in terms of the characteristic impedance Z_{os}, for an isolated single strip between parallel ground planes:

$$a/b = \frac{\eta}{4Z_{os}\sqrt{\epsilon_r}} - 0.441 \quad (13)$$

for $a/b>0.35$.

Similarly, for thin dual strips between parallel ground planes, the fringing capacitances (Fig. 5) are added to the parallel plate capacitances (3) and substituted in (1) to yield

$$c/b = (1 - g/b)\left(\frac{\eta}{4Z_{od}\sqrt{\epsilon_r}} - C_{c\infty}'/\epsilon\right) \quad (14)$$

for $(c/b)/(1-g/b)>0.35$, as the relation between relative strip width c/b, and the characteristic impedance, Z_{od}. Corrections for narrow strips will be given in the next section.

V. Considerations of Accuracy

If the strip widths a and c are allowed to become too small, then there is interaction of the fringing fields from the two edges, and the decomposition of total ca-

pacitance into parallel-plane capacitance and fringing capacitances (which are based on infinite strip widths), no longer is accurate. Cohn [1], [6] shows that for a single strip centered between parallel planes, the error in total capacitance from this cause is about 1.24 per cent for $w/(b-t)=0.35$, where w is the width of the strip, t is its thickness, and b is again the ground-plane spacing. If maximum error in total capacitance of approximately this magnitude is allowed, then it is necessary that $a/b>0.35$ and $[(c/b)/(1-g/b)]>0.35$.

Should these inequalities be too restricting, it is possible to make approximate corrections based on increasing the parallel-plate capacitance to compensate for the loss of fringing capacitance due to interaction of fringing fields. If an initial value, a_1/b is found to be less than 0.35, a new value, a_2/b can be used, where

$$a_2/b = (0.07 + a_1/b)/1.20 \tag{15}$$

provided $0.1<a_2/b<0.35$. A similar formula for correcting an initial value c_1/b, gives a new value, c_2/b as

$$c_2/b = [0.07(1 - g/b) + c_1/b]/1.20 \tag{16}$$

provided g/b is fairly small and $0.1<(c_2/b)/(1-g/b)<0.35$. These formulas are based on a linear approximation to the exact fringing capacitance of a single thin strip for a width to plate-spacing ratio between 0.1 and 0.35. As the relative strip width becomes narrower than 0.35, the fringing capacitance, defined as total capacitance less parallel plate capacitance, decreases from the value C_f' or $C_{c\infty}'$ used in the derivations and graphs. The total capacitance is given by substituting into (1) the exact thin-strip formula for Z_o given in [6]. Eqs. (15) and (16) add sufficient parallel-plate capacitance to compensate for the loss of fringing capacitance. The loss of fringing is assumed to vary linearly below a relative width of 0.35, and it is also assumed that $C_{c\infty}'$ decreases by the same amount as does C_f'. Although the formulas are analytically only approximate for coupled strips, they are sufficiently accurate for practical use because they do no more than give a small correction to a quantity that is reasonably close to the exact value. They can be used with both isolated and coupled strips.

The discontinuity in the slope of C_{ae}'/ϵ in Fig. 8 at $d/g=0$ is not a physical phenomenon, but is a mathematical result of considering dimension a to extend to the edge of strips c for positive d, while for negative d, dimension a extends to the edge of strip a, as shown in Fig. 3. The only practical effect of this situation is that the width of strip a is equal to dimension a when d is negative, but when d is positive the width of strip a is equal to the sum of dimensions a and d. This is shown clearly in Fig. 3.

In deriving the fringing capacitance, one of the assumptions made was that the strip was infinitely thin. Investigation of a graph given by Cohn [1], [6] shows that the fringing capacitance, C_f'/ϵ from a strip centered between parallel ground planes increases by about 2 per cent for a 1 per cent increase in the ratio of strip thickness to plate spacing, for a very thin strip. Fringing capacitance is usually only part of the total capacitance involved in a strip-line circuit, so that for many situations, a strip no thicker than 1 or 2 per cent of the associated parallel-plate separation can be considered thin without serious error.

The derivations for the fringing capacitances are exact for infinitely thin strips with dimension a (see Fig. 3) extending infinitely far to the right while dimension c extends infinitely far to the left. The computed values from which the curves were plotted were accurate to three places after the decimal, although the curves themselves cannot be relied on to be closer than about ± 5 in the third significant figure, as plotted.

For insertion of the strip a between strips c beyond the maximum plotted, $d/g=1.0$, the even-mode values C_{ae}'/ϵ and C_{ce}'/ϵ do not change from their values at $d/g=1.0$, while $\Delta C/\epsilon$ and the odd-mode values C_{ao}'/ϵ and C_{co}'/ϵ, can be found simply by adding $4(d/g-1)$ to their values at $d/g=1$. For spacing between strips c greater than $g/b=0.5$, or for a separation $d/g<-2.0$, probably some different strip-line construction would be more suitable.

Finally, it should be noted that if these curves predict a value of d positive and approximately equal to or greater than c, the result is not valid. When strip a protrudes all the way between strips c in this manner, it merely means that too great a value of g/b was selected to realize the odd-mode capacitance. This restriction may be expressed mathematically by requiring that $d<c-(g/2)$. If this condition is not met for a desired set of capacitances, then it is necessary to make g/b smaller and determine new dimensions.

VI. Applications

The graphs and procedures described above have been used to design strip-line 3-db couplers [1], [5].

A 3-db coupler was designed to have an input impedance of 50 ohms. Fig. 10 shows pertinent details of its construction. The dielectric material used, Rexolite #2200, has a published dielectric constant of 2.77. This material is commercially available with sheets of 0.001-inch copper bonded to the sides.

A center-frequency coupling value of -2.8 db, rather than -3.0 db, was chosen to allow for an expected decrease in coupling at frequencies away from the center frequency. Use of the formulas of [1] or [5] gave values of 125.15 ohms for Z_{oe} and 19.95 ohms for Z_{oo}. Substitution of these values in (1) gave $C_{oe}/\epsilon=1.81$ and $C_{oo}/\epsilon=11.34$. Using the laminate thicknesses shown on Fig. 10, it was found that $g/b=0.0964$. Eq. (9) and Fig. 4 showed the required value of d/g to be 0.445. Then, use of the procedure described in the preceding section, including Eqs. (11) and (12), gave $a/b=0.284$ and $c/b=0.107$. (In the coupler constructed, a value of 0.097 was used for c/b because Fig. 5 had not been pre-

pared, and an approximate method was used to find $C_{e\infty}'/\epsilon$.) The coupler was made one-quarter wavelength long in the dielectric at the center frequency of 200 Mc.

Performance curves for this coupler are shown in Fig. 11. The behavior of the coupler is typical of 3-db backward couplers made in other configurations.

A second 3-db coupler was made on another project for parametric amplifier work. This coupler was designed to have a center frequency of 1000 Mc. In this design the strip widths were widened in accordance with (15) and (16) for correcting narrow strips. The dimensions are shown in Fig. 12. The bulk of input reflections were caused by reactance of the right-angle bends joining the feed lines to the coupling region. The purely capacitive tuning screws shown were much more effective in cancelling the reflections than were modifications of the structure of the bend or tabs on the feed lines at the bends. The greater effect of the bend reactance as frequency increases is shown in the performance curves for this coupler, Fig. 13. Fig. 14 is a photograph of the coupler.

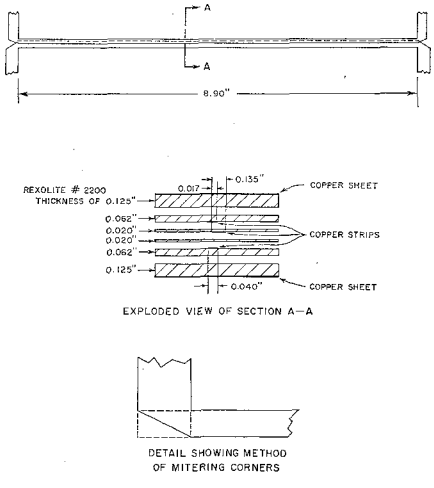

Fig. 10—Details of construction of 200-Mc 3-db backward coupler.

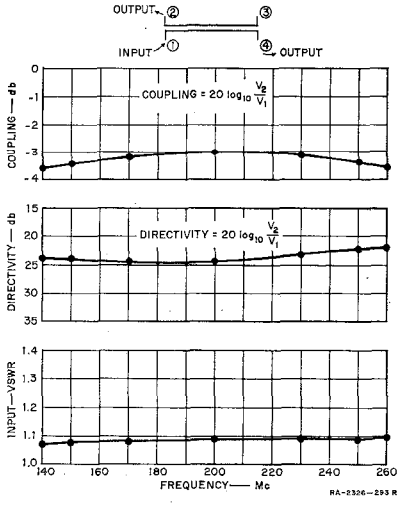

Fig. 11—Performance of 200-Mc 3-db backward coupler.

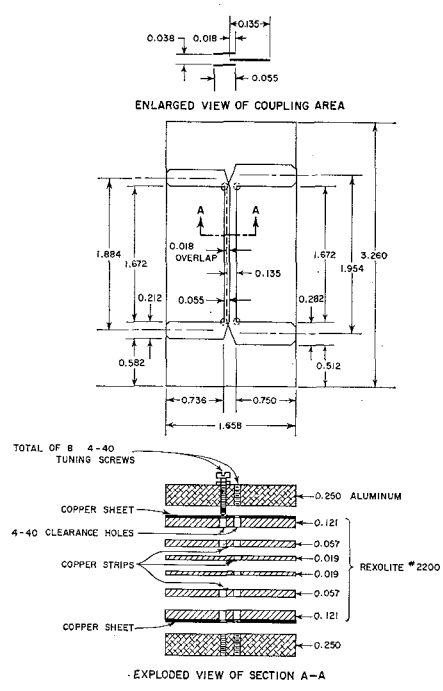

Fig. 12—Details of construction of 1000-Mc 3-db backward coupler.

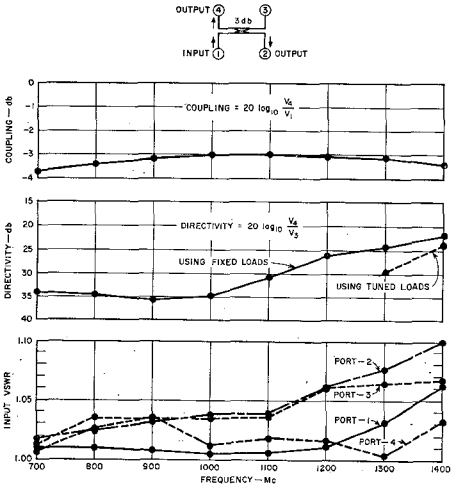

Fig. 13—Performance of 1000-Mc 3-db backward coupler.

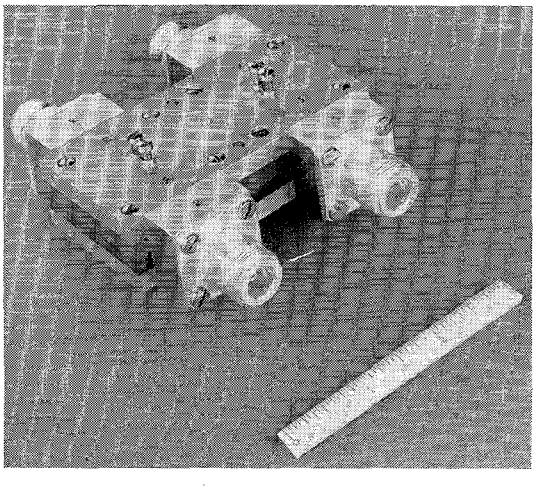

Fig. 14—1000-Mc 3-db backward coupler.

Appendix

Derivation of Fringing Capacitances

A. Preliminary

It is desired to determine the static fringing capacitances shown on the structure of Fig. 3 by means of conformal mapping techniques [7], [8]. This can be done by subjecting the boundaries of the structure to transformations under which capacitance is invariant, and that lead to a new structure for which capacitance is known. Subtraction of parallel-plate capacitances of the original structure from the total capacitance then leaves the fringing capacitances. The analysis will be limited to structures in which strips c and a are so wide that interaction between fringing fields of the two edges of a single strip are negligible. As discussed in Section V, this requires that the approximate relations $a/b > 0.35$ and $[(c/b)/(1-g/b) > 0.35]$ be held. Under these conditions it is possible to let strip c extend infinitely far to the left, and strip a infinitely far to the right without disturbing the fringing fields appreciably in the region where the two strips interact. Also, the electric field can lie parallel to the horizontal center line where no conductor exists, but cannot cross it because of the symmetry of the structure, assuming the two conducting strips c are always at the same potential with respect to each other. Therefore a magnetic wall can be placed along the center line extending infinitely far to the left from the left edge of strip a. These modifications allow analysis of only half of the total symmetrical structure, as shown in Fig. 15(a). The mathematical model is shown in Fig. 15(b). Conductors are indicated by solid lines, and the magnetic wall is indicated by a dashed line. The upper-case script letters of Fig. 15(b) denote pertinent points of the structure and will serve as references when transformations to different complex planes are made. The values chosen for the various points on the z plane will prove convenient under transformation.

The analysis consists essentially in transforming the contours of the structure on the z plane into a parallel-plate representation on the w plane, where capacitance can be computed directly. This procedure is complicated by having three conductors while only two are desired for a parallel-plate representation. This complication will be resolved by showing that there exists a surface of zero potential, which can be replaced by an electric wall, running between the conducting strips for the odd mode, and that this same surface can be treated as a magnetic wall for the even mode. Fig. 15(c) shows the wall running between points $\mathcal{G}$, a saddle-point, and $\mathcal{K}$, following some curve whose exact shape is unknown. A subsequent transformation will rectify this curve, dividing the structure into two parts, each of which has only two conductors and can be further analyzed separately.

As a first step, the interior of the polygon $\mathcal{A}\mathcal{B}\mathcal{C}\mathcal{D}\mathcal{A}'$ will be mapped onto the upper half of a z_1 plane as shown in Fig. 16(a). The mapping is given by Kober [9] as

$$z = \frac{1-\alpha}{2} \ln (z_1 - 1) + \frac{1+\alpha}{2} \ln (z_1 + 1). \qquad (17)$$

The points noted on the z plane are related to points on the real axis of the z_1 plane by

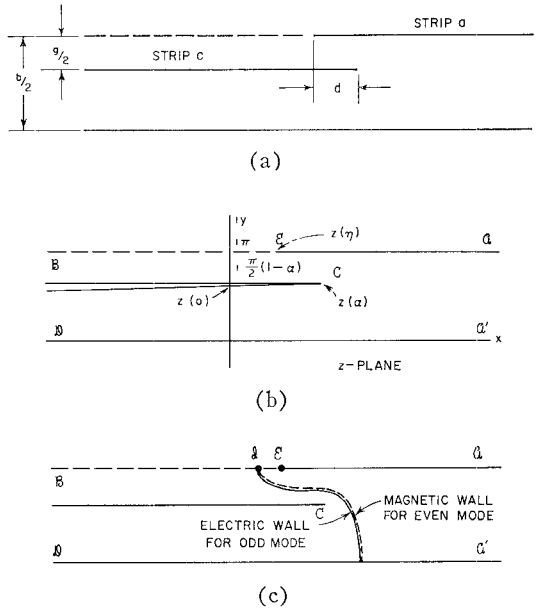

Fig. 15—Cross section of proposed configuration on z plane.

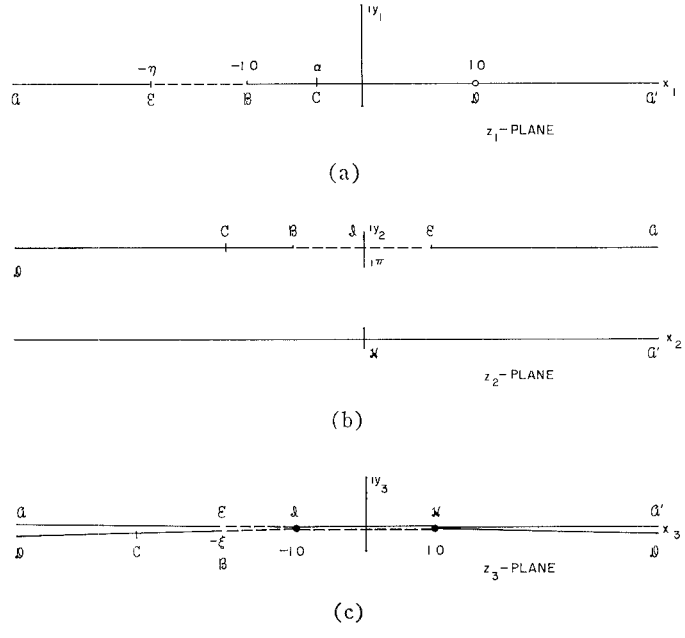

Fig. 16—Intermediate transformations from z plane.

$$z(0) = i\frac{\pi}{2}(1-\alpha)$$

$$z(\alpha) = \frac{1-\alpha}{2}\ln(1-\alpha) + \frac{1+\alpha}{2}\ln(1+\alpha) + i\frac{\pi}{2}(1-\alpha)$$

$$z(\eta) = \frac{1-\alpha}{2}\ln(1+\eta) + \frac{1+\alpha}{2}\ln(\eta-1) + i\pi. \quad (18)$$

Notice that

$$\eta > 1.0$$
$$-1.0 < \alpha < 1.0. \quad (19)$$

The small circle at point $\mathfrak{D}$ indicates an infinitely small gap at that point, such that the conductors on either side may be at different potentials. Point $\mathfrak{D}$ is removed to $-\infty$ under the next transformation, which is to a z_2 plane. This transformation will place points $\mathfrak{B}$ and $\mathfrak{E}$ equidistant from the y_2 axis, as shown in Fig. 16(b). The transformation is

$$z_1 = 1 + \sqrt{2(\eta+1)}\, e^{z_2}. \quad (20)$$

The source of this transformation, as with most transformations used in this chapter, is a combination of experience and the use of references [7]–[10]. However, although the derivations of the transformations may not be obvious, they may be checked at points of interest simply by substituting values of the independent variable and observing that the transformation gives the correct result for the dependent variable.

The structure on the z_2 plane will now be related to the given structure. The conductor between $\mathfrak{A}'$ and $\mathfrak{D}$ corresponds to the ground plane on the given structure. The conductor between $\mathfrak{A}$ and $\mathfrak{E}$ corresponds to strip a in the given structure, and the conductor between $\mathfrak{B}$ and $\mathfrak{D}$ corresponds to one of the strips c in the given structure. The z_2 plane structure is symmetrical about the y_2 axis. Under even-mode excitation both conducting strips a and c are at the same potential, and thus no electric field lines cross the y_2 axis. Therefore, a magnetic wall can be placed along the y_2 axis and left and right halves may be analyzed separately. Under odd-mode excitation the conducting strips a and c are oppositely charged with respect to the ground plane, and thus all electric field lines crossing the y_2 axis must cross normal to that axis to preserve symmetry. Therefore, an electric wall at zero potential may be placed along the y_2 axis and left or right half only need be analyzed. Notice that script letters $\mathfrak{K}$ and $\mathfrak{J}$ have been assigned to the end points of the line of symmetry. By means of the transformation

$$z_2 = \text{arc cosh } z_3 \quad (21)$$

the interior of the polygon $\mathfrak{A}\mathfrak{J}\mathfrak{K}\mathfrak{A}'$ goes into the upper half of the z_3 plane, and the polygon $\mathfrak{J}\mathfrak{D}\mathfrak{K}$ goes into the lower half of the z_3 plane, as shown in Fig. 16(c). Only that portion of the x_3 axis between $\mathfrak{J}$ and $\mathfrak{K}$ is common to both upper and lower half-planes, and for this reason the x_3 axis is shown split beyond $\mathfrak{K}$ and $\mathfrak{J}$. The solid line (conductor) between $\mathfrak{K}$ and $\mathfrak{J}$ is to be used for odd-mode analysis, while the dashed line (magnetic wall) is to be used for even-mode analysis.

On the z_3 plane $\mathfrak{K}$ and $\mathfrak{J}$ fall at $+1.0$ and -1.0, as can be determined by subsituting the known values of $\mathfrak{K}$ and $\mathfrak{J}$ on the z_2 plane into (21). In order to find $z_3(\mathfrak{B})$ it is necessary to work from the z_1 plane, where Kober [9] shows that $z_1(\mathfrak{B}) = -1.0$. Then, by successive substitution and manipulation of (20) and (21), it is found that

$$z_3(\mathfrak{B}) = -\frac{1}{2}\left[\frac{2}{\sqrt{2(\eta+1)}} + \frac{\sqrt{2(\eta+1)}}{2}\right] = -\xi \quad (22)$$

where $-\xi$ is the value of $z_3(\mathfrak{B})$ on the z_3 plane. Notice that

$$\xi > 1.0. \quad (23)$$

By the symmetry of the z_2 plane with respect to the imaginary axis and the nature of the transformation (21),

$$z_3(\mathfrak{E}) = z_3(\mathfrak{B}) = -\xi \quad (24)$$

although it should be noted that $\mathfrak{E}$ and $\mathfrak{B}$ are on opposite sides of a branch cut on the z_3 plane.

B. Odd-Mode Fringing Capacitance—Strip a

Now consider the odd mode, and investigate the fringing capacitance of strip a, which is associated with point $\mathfrak{E}$. The upper half of the z_3 plane is transformed to a parallel plate region on the w_1 plane by

$$z_3 = (\tfrac{1}{2})[(\xi-1)\cosh \pi w_1 - (\xi+1)] \quad (25)$$

as shown on Fig. 17(a).

The total capacitance on the w_1 plane is parallel-plate capacitance. The amount of capacitance per unit permittivity between the w_1-plane origin and some location $u_1 > 0$ is equal to u_1, for unit depth into the paper, because there is unit spacing between the conducting planes. This is the odd-mode capacitance to one ground plane from strip a. The corresponding capacitance for strip a on the z plane is the fringing capacitance from the vicinity of $\mathfrak{E}$ plus the parallel-plate capacitance, which will be defined as the amount of parallel-plate capacitance from strip a to ground, measured between $z(\alpha)$ (Edge $\mathfrak{C}$) and the mapping of u_1 mentioned above onto the z plane. Mathematically, the z-plane parallel-plate capacitance, relevant to some value u_1 on the w_1 plane, has the value $(1/\pi)Re[z(u_1) - z(\alpha)]$, as can be deduced from Fig. 15(b). Alternatively this defines the fringing capacitance in the odd

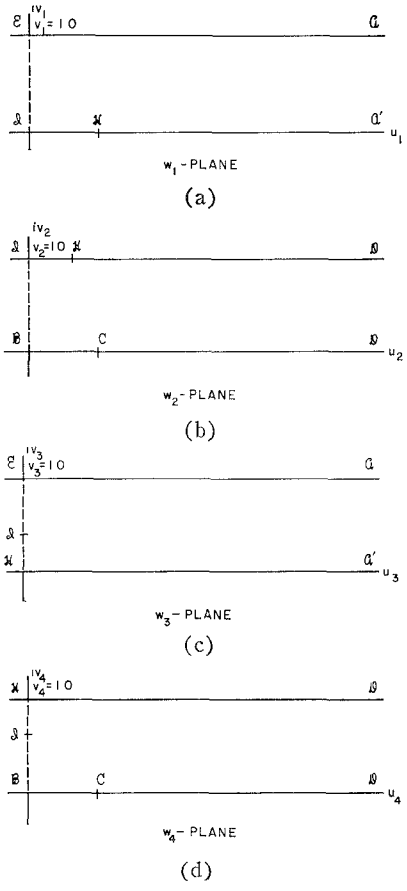

Fig. 17—Final configurations on w planes

mode from strip a to one ground plane as the difference between the total capacitance to some value u_1 on the w_1 plane and the parallel-plate capcitance out to the mapping of u_1 on the z plane, as u_1 approaches infinity. This odd-mode fringing capacitance from strip a will be denoted by C_{ao}'/ϵ. From the above discussion,

$$C_{ao}'/\epsilon = \lim_{u_1 \to \infty} \left\{ u_1 - \operatorname{Re} \frac{1}{\pi} [z(u_1) - z(\alpha)] \right\}. \quad (26)$$

From a physical point of view, this definition of parallel-plane capacitance assumes that strips a and c always overlap. Mathematically, the definition of parallel-plane capacitance is wholly arbitrary, so that this physical defect in definition need not be ameliorated until the mathematical derivation is complete. When the proper substitutions have been made in (26), allowing the approach to the limit to take place, sufficient manipulation gives the final expression for C_{ao}'/ϵ as

$$C_{ao}'/\epsilon = \operatorname{Re} \frac{1}{\pi} \left[z(\alpha) - \ln \frac{(\eta + 3) - 2\sqrt{2(\eta + 1)}}{4} \right]. \quad (27)$$

C. Odd-Mode Fringing Capacitance—Strip c

Strip c is associated with points $\mathfrak{B}\mathfrak{C}\mathfrak{D}$. Eq. (21) mapped the polygon $\mathfrak{D}\mathfrak{K}\mathfrak{J}\mathfrak{G}\mathfrak{D}$ of the z_2 plane onto the lower half of the z_3 plane (Fig. 16). The lower half of the z_3 plane is next mapped onto the w_2 plane by means of the transformation

$$z_3 = -\tfrac{1}{2}[(\xi + 1) + (\xi - 1) \cosh \pi\omega_2]. \quad (28)$$

Assuming unit depth into the paper, the total capacitance per unit permittivity as a function of u_2 is equal to u_2. The parallel-plate capacitance to the adjacent ground plane of one of the strips c may be defined as

$$\frac{\operatorname{Re}[z(\alpha) - z(u_2)]}{(\pi/2)(1 - \alpha)},$$

from Fig. 15, in a manner similar to that defined for strip a. The difference between total capacitance and parallel-plate capacitance, relevant to some value of u_2 approaching infinity, is the odd-mode fringing capacitance of strip c, and will be denoted by C_{co}'/ϵ. Therefore, from the above discussion,

$$C_{co}'/\epsilon = \lim_{u_2 \to \infty} \left\{ u_2 - \operatorname{Re} \frac{[z(\alpha) - z(u_2)]}{(\pi/2)(1 - \alpha)} \right\}. \quad (29)$$

Again, substitution, passing to the limit, and manipulation yields the final result.

$$C_{co}'/\epsilon = \operatorname{Re} \frac{1}{\pi} \left[\frac{1 + \alpha}{1 - \alpha} \ln 2 + \ln \frac{8(\eta + 1)}{(\eta + 3) - 2\sqrt{2(\eta + 1)}} - \frac{2}{1 - \alpha} z(\alpha) \right]. \quad (30)$$

D. Even-Mode Fringing Capacitance-Strip a

In analyzing the even mode, the two strips, a and c are at the same potential, as previously discussed, and the plane $\mathfrak{J}\mathfrak{K}$ may be considered as a magnetic wall. For strip a, associated with point $\mathfrak{E}$, the transformation from the upper half of the z_3 plane, Fig. 15(c) to a w_3 plane, Fig. 16(c), is

$$z_3 = (1/2)[(\xi + 1) \cosh \pi\omega_3 - (\xi - 1)]. \quad (31)$$

The definition and discussion of parallel-plate capacitance for strip a given in connection with odd-mode capacitance holds for this case also. The even-mode fringing capacitance is given by the difference between total capacitance and parallel-plate capacitance, so that by analogy with (26), the even-mode fringing capacitance for strip a is

$$C_{ae}'/\epsilon = \lim_{u_3 \to \infty} \{ u_3 - \operatorname{Re} (1/\pi)[z(u_3) - z(\alpha)] \}. \quad (32)$$

The substitutions and manipulations are much like those used to find C_{ao}'/ϵ. The result is

$$C_{ae}'/\epsilon = \operatorname{Re} \frac{1}{\pi} \left[z(\alpha) - \ln \frac{(\eta + 3) + 2\sqrt{2(\eta + 1)}}{4} \right]. \quad (33)$$

E. Even-Mode Fringing Capacitance—Strip c

The same reasoning and procedure may be used in finding the even-mode fringing capacitance from strip c as were used for the other three fringing capacitances

and, in fact, this was done in the original work on this problem. However, only three capacitances are required to describe a parallel coupled TEM structure, as in Fig. 2, and this indicates the possibility that if three fringing capacitances are known, the fourth may be related to them by a function which is independent of the geometry of the structure. This geometry-independent function, applicable to any parallel-coupled TEM structure that can be represented schematically by Fig. 2, is given by (6), which upon manipulation may be written as

$$C_{ce}'/\epsilon = C_{co}'/\epsilon - C_{ao}'/\epsilon + C_{ae}'/\epsilon = C_{co}'/\epsilon - \Delta C/\epsilon, \quad (34)$$

using (7) for the definition of $\Delta C/\epsilon$. Thus, the unkown fringing capacitance, C_{ce}'/ϵ, can be written as a linear combination of the other three fringing capacitances. Substitution of (27), (30), and (33) into (34) yields

$$C_{ce}'/\epsilon = \operatorname{Re}\frac{1}{\pi}\left[\frac{1+\alpha}{1-\alpha}\ln 2 - \frac{2}{1-\alpha}z(\alpha) + \ln\frac{8(\eta+1)}{(\eta+3)+2\sqrt{2(\eta+1)}}\right]. \quad (35)$$

This result agrees with that found for C_{ce}'/ϵ directly from the mapping.

F. Definition of Parallel-Plate Capacitance of Strip a

In mathematically determining the fringing capacitances for the centered center-strip, strip a, the equivalent parallel-plate capacitor on the z plane, Fig. 15, is extended to the right from $z(\alpha)$ for all cases. In considering the physics of the situation, it is apparent that a more realistic definition would have the parallel-plate capacitance for strip a computed from the edge of strip a, $z(\eta)$, except when strip a is shielded by strip c, and then the parallel-plate capacitance would be computed from the edge of the shielding strip c at $z(\alpha)$. In order for the plotted curves to agree with this physical definition, it was necessary to add a parallel-plate capacitance to computed values of C_{ao}'/ϵ and C_{ae}'/ϵ. This parallel-plate capacitance was added only when $z(\eta) > z(\alpha)$, and simply replaced that subtracted in the derivation. The value added to C_{ao}'/ϵ and C_{ae}'/ϵ was equal to $[z(\eta) - z(\alpha)]/\pi$. In terms of dimensions, this additional capacitance per unit permittivity can be expressed as $|2d/b|$ for $d<0$. The plotted curves for strip a, Figs. 8 and 9, incorporate this term.

G. Derivation of $C_{c\infty}'/\epsilon$

The fringing capacitance $C_{c\infty}'/\epsilon$ is that from the edge of a strip located between a parallel magnetic wall and a parallel electric wall, as indicated on the graph, Fig. 5. It can be specified mathematically as

$$C_{c\infty}'/\epsilon = \lim_{d\to-\infty} C_{co}'/\epsilon \quad \text{or} \quad C_{ce}'/\epsilon. \quad (36)$$

From Fig. 15 it can be seen that $z(\eta)\to\infty$ as $d\to-\infty$, and on Fig. 16(a) this corresponds to $\eta\to\infty$. Thus, using (30),

$$C_{c\infty}'/\epsilon = \lim_{\eta\to\infty} \operatorname{Re}\frac{1}{\pi}\left[\frac{1+\alpha}{1-\alpha}\ln 2 + \ln\frac{8(\eta+1)}{(\eta+3)-2\sqrt{2(\eta+1)}} - \frac{2}{1-\alpha}z(\alpha)\right] \quad (37)$$

or

$$C_{c\infty}'/\epsilon = \frac{1}{\pi}\left[\frac{1+\alpha}{1-\alpha}\ln 2 + \ln 8 - \frac{2}{1-\alpha}\operatorname{Re} z(\alpha)\right]. \quad (38)$$

The real part of $z(\alpha)$ is given in (18), and from Fig. 15, α is found to be related to g/b by

$$\alpha = 2g/b - 1. \quad (39)$$

Thus, $C_{c\infty}'/\epsilon$ can be expressed in terms of g/b by

$$C_{c\infty}'/\epsilon = \frac{1}{\pi}\left[2\ln 2 - \ln(1-g/b) - \frac{g/b}{1-g/b}\ln g/b\right]. \quad (40)$$

This is plotted in Fig. 5. The fringing capacitance C_f'/ϵ is the value of $C_{c\infty}'/\epsilon$ for $g/b=0$, and is

$$C_f'/\epsilon = \frac{2}{\pi}\ln 2 = 0.4413. \quad (41)$$

Acknowledgment

The author wishes to express his appreciation to Dr. G. L. Matthaei, who suggested the problem analyzed herein, for his encouragement and technical guidance during the course of this work.

Bibliography

[1] J. K. Shimizu and E. M. Jones, "Coupled-Transmission-Line directional couplers," IRE Trans. on Microwave Theory and Techniques, vol. MTT-6, pp. 403–410; October, 1958.

[2] S. B. Cohn, *et al.*, "Research on Design Criteria for Microwave Filters," Stanford Res. Inst., Menlo Park, Calif., Final Rept., SRI Project 1331, Contract No. DA 36-039 SC-64625; 1957.

[3] G. L. Matthaei, "Design of wide-band (and narrow-band) band-pass microwave filters on the insertion loss basis," IRE Trans. on Microwave Theory and Techniques, vol. MTT-8, pp. 580–593; November, 1960.

[4] B. M. Oliver, "Directional electromagnetic couplers," Proc. IRE, vol. 42, pp. 1686–1692; November, 1954.

[5] E. M. T. Jones and J. T. Bolljahn, "Coupled-Strip-Transmission-Line filters and directional couplers," IRE Trans. on Microwave Theory and Techniques, vol. MTT-4, pp. 75–81; April, 1956.

[6] S. B. Cohn, "Problems in strip transmission lines," IRE Trans. on Microwave Theory and Techniques, vol. MTT-3, pp. 119–126; March, 1955.

[7] W. R. Smythe, "Static and Dynamic Electricity," McGraw-Hill Book Co., Inc., New York, N. Y., ch. 4; 1939.

[8] Ernst Weber, "Mapping of Fields" in "Electromagnetic Fields: Theory and Applications," John Wiley and Sons, Inc., New York, N. Y., vol. 1; 1950.

[9] H. Kober, "Dictionary of Conformal Representations," Dover Publications, Inc., New York, N. Y., sec. 12.5, p. 155; 1952.

[10] R. V. Churchill, "Introduction to Complex Variables and Applications," McGraw-Hill Book Co., Inc., New York, N. Y., Appendix II; 1948.

[11] S. B. Cohn, "Shielded coupled-strip transmission line," IRE Trans. on Microwave Theory and Techniques, vol. MTT-3, pp. 29–38; October, 1955.